Journal of Environmental Science and Engineering A 6 (2017) 308-312
doi:10.17265/2162-5298/2017.06.004

The Buckling Behavior of Boron Nitride Nanotubes under Bending: An Atomistic Study

Van-Trang Nguyen

Department of Mechanical Design and Manufacture, Faculty of Mechanical Engineering, Thai Nguyen University of Technology, Thai Nguyen City 250000, Vietnam

Abstract: In this paper, the buckling behavior of zigzag BN (Boron Nitride) nanotubes under bending is studied through molecular dynamics finite element method with Tersoff potential. The tube with namely (15, 0) BN zigzag tube is investigated. The critical bending buckling angle, moment and curvature are studied and examined with respect to the tube length-diameter ratios from 5 to 30. Effects of a SW (Stone-Wales) defect in the middle tube on the bending behavior are also discussed. The results show that the tube length affects significantly the bending behavior of these tubes. All tubes exhibit brittle fracture under bending. The buckling takes place at the middle in the compressive side of these tubes. These results are important information on the buckling behaviors of pristine and Stone-Wales BN nanotubes, which will be useful for their future applications.

Key words: Atomistic simulation, bending, boron nitride nanotube, buckling.

1. Introduction

A BN-NT (Boron Nitride Nanotube) can be geometrically formed by rolling up a hexagonal BN layer or as a CNT (Carbon Nanotube) [1] in which alternating B and N atoms entirely substitute for C atoms as shown in Fig. 1.

Various techniques have been used to synthesize BN-NTs, including arc-discharge, chemical vapor deposition, laser ablation and ball milling methods [2]. BN-NTs exhibit good mechanical properties with high elastic modulus of ~0.5-1 TPa and tensile strength of ~61 GPa [3]. BN-NTs possess distinguishable chemical and thermal stability with high oxidation resistance up to 900 ºC in air [4], wide band-gaps independent of tube structures [5, 6] and excellent thermal conductivity [7]. BN-NTs are also an effective violet and ultra-violet light emission material [8, 9]. Potential applications of BN-NTs include nanofillers in polymeric [10] and metallic [11] composites, optoelectronic fields [8], radiation shielding in space vehicles [12]. Potential applications of BN-NTs need a comprehension of the mechanical properties and performance of BN-NTs under various loading conditions. BN-NTs under compression [13-15], tension [16, 17], torsion [16, 18-20] and bending with 2 fixed or simple supports [21, 22] have been investigated. So far, theoretical studies of the buckling behavior under bending of BN-NTs seem still unexplored. It should be noted that the buckling behavior of CNTs under bending has been investigated by continuum methods, atomistic simulations and multi-scale approach [23, 24]. In this paper, the buckling behavior of (15, 0) zigzag BN nanotubes under bending is studied through molecular dynamics finite element method with Tersoff potential. The critical bending buckling angle, curvature and moment are studied with respect to the length-diameter ratios of BN-NTs. Effects of a SW (Stone-Wales) defect in the middle tube on the bending behavior are also discussed.

Corresponding author: Van-Trang Nguyen, master, main research field: mechanic of material.

2. Framework for Analysis

Tersoff potential is used to model the B-N interatomic interactions [25]. The potential energy E of

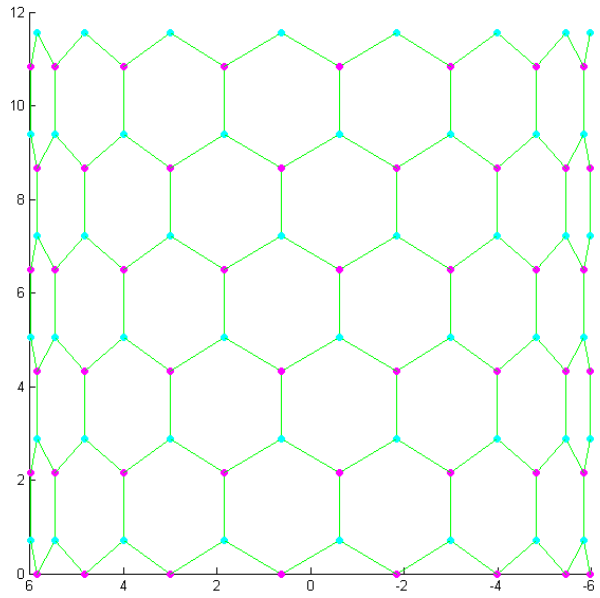

Fig. 1 Schematic illustration of (15, 0) BN zigzag tube.

the atomic structure is a function of atomic coordinates as Eqs. (1)-(10).

$$E = \sum_i E_i = \frac{1}{2}\sum_{i \neq j} V_{ij} \quad (1)$$

$$V_{ij} = f_C(r_{ij}) f_R(r_{ij}) + b_{ij} f_A(r_{ij}) \quad (2)$$

$$f_R(r_{ij}) = A_{ij} \exp(-\lambda_{ij}^I r_{ij}) \quad (3)$$

$$f_A(r_{ij}) = -B_{ij} \exp(-\lambda_{ij}^{II} r_{ij}) \quad (4)$$

$$f_C(r_{ij}) = \begin{cases} 1, r_{ij} \leq R_{ij} \\ \frac{1}{2} + \frac{1}{2}\cos\left(\pi \frac{r_{ij} - R_{ij}}{S_{ij} - R_{ij}}\right), R_{ij} \leq r_{ij} \leq S_{ij} \\ 0, r_{ij} \geq S_{ij} \end{cases} \quad (5)$$

$$b_{ij} = \chi_{ij}(1 + \beta_i^{n_i} \xi_{ij}^{n_i})^{-1/2n_i} \quad (6)$$

$$\xi_{ij} = \sum_{k \neq i,j} f_C(r_{ik}) \omega_{ik} g(\theta_{ijk}) \quad (7)$$

$$g(\theta_{ijk}) = 1 + \frac{c_i^2}{d_i^2} - \frac{c_i^2}{\left[d_i^2 + (h_i - \cos\theta_{ijk})^2\right]} \quad (8)$$

$$\lambda_{ij}^I = \frac{\lambda_i^I + \lambda_j^I}{2};\ \lambda_{ij}^{II} = \frac{\lambda_i^{II} + \lambda_j^{II}}{2};\ A_{ij} = \sqrt{A_i A_j} \quad (9)$$

$$B_{ij} = \sqrt{B_i B_j};\ R_{ij} = \sqrt{R_i R_j};\ S_{ij} = \sqrt{S_i S_j} \quad (10)$$

Here, the lower indices i, j and k label the atoms of the system, where interaction between atoms i and j is modified by a third atom k. r_{ij} is the distance between atoms i and j; f_A and f_R are the attractive and repulsive pairwise terms; f_C is a cutoff function to ensure the nearest-neighbor interactions; R_{ij} and S_{ij} denote the small cutoff distance and the large one, respectively; B_{ij} is a bond-order parameter, depending on the local coordination of atoms around atom i. Further detail of the Tersoff potential is given by Tersoff, J. [25]. Force field parameters are taken from the work by Sevik, C., et al. [26] for B-N interactions. While DFT (Density Functional Theory) calculations and MD (Molecular Dynamics) simulations are time-consuming, MDFEMs (Molecular Dynamic Finite Element Methods), sometime known as atomic-scale finite element methods or atomistic finite element methods, have been developed to analyze nanostructured materials in a computationally efficient way [27, 28]. To achieve the atomic positions of the BN-NT under specific boundary conditions, MDFEM is here adopted. In MDFEM, atoms and atomic displacements are considered as nodes and translational degrees of freedom (nodal displacements), respectively. Both first and second derivatives of system energy are used in the energy minimization computation, hence, it is faster than the standard conjugate gradient method which uses only the first order derivative of system energy as discussed by Liu, B., et al. [27]. The stiffness matrices of these elements are established based upon interatomic potentials. Similar to conventional finite element method, global stiffness matrix is assembled from element stiffness matrices. Hence, relations between atomic displacement and force can be derived by solving a system of equations. Further detailed numerical procedure of MDFEM and specific development for Tersoff potentials are available in the previous work by Le, M. Q. and Nguyen, D. T. [29] and references therein. Initial positions of atoms are generated by using the B-N bond length of 1.444 Å taken from previous MD simulations [30] at optimized structure at 0 K with the same force field. (15, 0) BN zigzag tube with tube diameter about 1.194 is considered.

3. Results and Discussion

Fig. 2 shows the variations of the bending moment versus the bending angle of pristine and SW (15, 0) BN tubes with the length-diameter ratio L/D = 20. The bending angle θ is here defined as the angle between 2

planes containing the 2 ends of the tube under bending. It can be seen from Fig. 2 that the bending moment increases monotonously with an increase of the bending angle up to a critical value, and then the bending moment drops suddenly, demonstrating a brittle fracture.

The critical bending angle of the pristine (15, 0) BN tube is approximately 27.5°, 58.5°, 88.3°, 118.1° and 176.6° for L/D = 5, 10, 15, 20 and 30, respectively. The critical bending angle of the SW (15, 0) BN tube on tensile side is approximately 20.6°, 37.8°, 57.3°, 73.4° and 122.7°, for L/D = 5, 10, 15, 20 and 30, respectively. The critical bending angle of the SW (15, 0) BN tube on compressive side is approximately 28.7°, 56.2°, 84.8°, 110.1° and 169.7°, for L/D = 5, 10, 15, 20 and 30, respectively.

Fig. 3 shows the effects of tube's length on the variations of the critical bending moments of pristine and SW BN tubes. The critical bending moment of pristine and SW on compressive side (15, 0) BN tubes increases with an increase of the tube's length in the range L/D = 5-30.

Fig. 4 shows the effects of tube's length on the variations of the critical bending angle of pristine and SW BN tubes. The critical bending angles of these 2 tubes increase with increasing the tube's length.

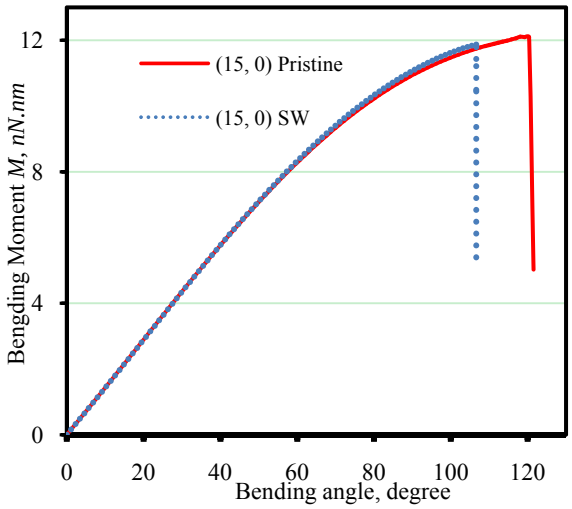

Fig. 2 Variations of the bending moment versus the bending angle of the pristine and SW (15, 0) BN tubes with L = 20D.

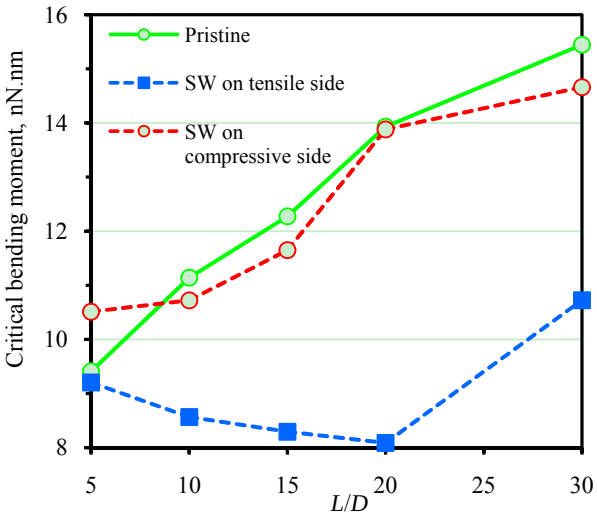

Fig. 3 Variations of the critical bending moment versus the tube length of pristine and SW(15, 0) BN tubes.

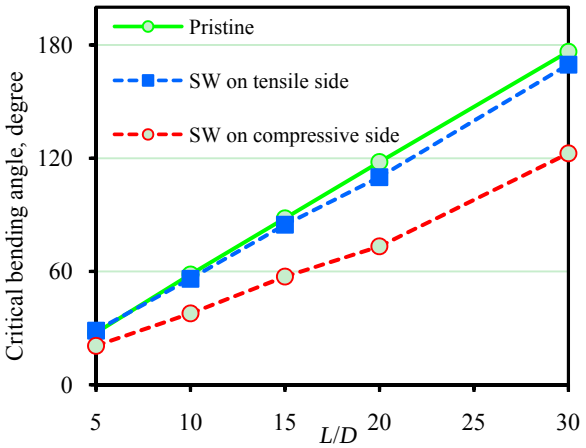

Fig. 4 Variations of the critical bending angle versus the tube length of pristine and SW (15, 0) BN tubes.

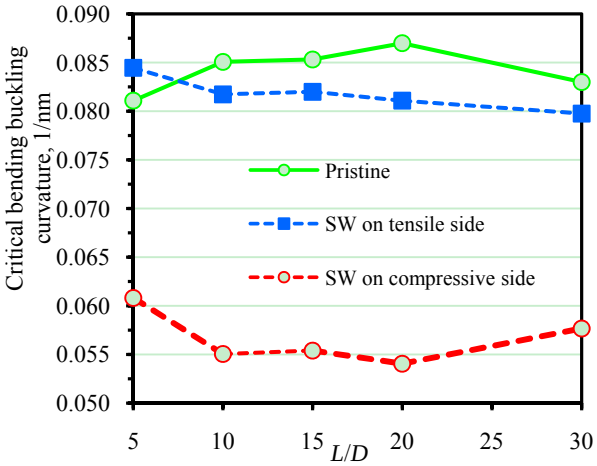

Fig. 5 Variations of the critical bending buckling curvature versus the tube length of pristine and SW (15, 0) BN tubes.

Fig. 5 shows the effects of tube's length on the variations of the critical bending buckling curvature of pristine and SW BN tubes. The critical bending buckling curvature of SW (15, 0) BN tube decreases with increasing the tube's length and the critical bending buckling curvature of pristine (15, 0) BN tube increases with increasing the tube's length for the tube's length in the range L/D = 5-20. However, with the tube's length in the range L/D = 20-30, the critical bending buckling curvature of SW on compressive side (15, 0) BN tubes increases.

5. Conclusions

The present work investigates the simulation results of the buckling behavior of zigzag pristine and SW BN nanotubes under bending with the use of MDFEM. The main points can be summarized that the tube length affects significantly the bending behavior of these tubes. All tubes exhibit brittle fracture under bending. The buckling takes place at the middle in the compressive side of these tubes. More investigations should be done to analyze in detail the buckling behavior of the BN tubes.

Acknowledgements

Van-Trang Nguyen was supported by the Thai Nguyen University of Technology, Thai Nguyen University, Vietnam.

References

[1] Iiiima, S. 1991. "Helical Microtubules of Graphitic Carbon." *Nature* 354 (6348): 56-8.

[2] Zhi, C., Bando, Y., Tang, C., and Golberg, D. 2010. "Boron Nitride Nanotubes." *Materials Science and Engineering: R: Reports* 70 (3): 92-111.

[3] Arenal, R., Wang, M. S., Xu, Z., Loiseau, A., and Golberg, D. 2011. "Young Modulus, Mechanical and Electrical Properties of Isolated Individual and Bundled Single-Walled Boron Nitride Nanotubes." *Nanotechnology* 22 (26): 265704.

[4] Chen, Y., Zou, J., Campbell, S. J., and Le Caer, G. 2004. "Boron Nitride Nanotubes: Pronounced Resistance to Oxidation." *Applied Physics Letters* 84 (13): 2430-2.

[5] Baumeier, B., Krüger, P., and Pollmann, J. 2007. "Structural, Elastic and Electronic Properties of SiC, BN and BeO Nanotubes." *Physical Review B* 76 (8): 085407.

[6] Guo, G. Y., Ishibashi, S., Tamura, T., and Terakura, K. 2007. "Static Dielectric Response and Born Effective Charge of BN Nanotubes from ab Initio Finite Electric Field Calculations." *Physical Review B* 75 (24): 245403.

[7] Chang, C. W., Fennimore, A. M., Afanasiev, A., Okawa, D., Ikuno, T., Garcia, H., et al. 2006. "Isotope Effect on the Thermal Conductivity of Boron Nitride Nanotubes." *Physical Review Letters* 97 (8): 085901.

[8] Attaccalite, C., Wirtz, L., Marini, A., and Rubio, A. 2013. "Efficient Gate-Tunable Light-Emitting Device Made of Defective Boron Nitride Nanotubes: From Ultraviolet to the Visible." *Scientific Reports* 3.

[9] Li, L. H., Chen, Y., Lin, M. Y., Glushenkov, A. M., Cheng, B. M., and Yu, J. 2010. "Single Deep Ultraviolet Light Emission from Boron Nitride Nanotube Film." *Applied Physics Letters* 97 (14): 141104.

[10] Meng, W., Huang, Y., Fu, Y., Wang, Z., and Zhi, C. 2014. "Polymer Composites of Boron Nitride Nanotubes and Nanosheets." *Journal of Materials Chemistry C* 2 (47): 10049-61.

[11] Nautiyal, P., Gupta, A., Seal, S., Boesl, B., and Agarwal, A. 2017. "Reactive Wetting and Filling of Boron Nitride Nanotubes by Molten Aluminum during Equilibrium Solidification." *Acta Materialia* 126: 124-31.

[12] Kang, J. H., Sauti, G., Park, C., Yamakov, V. I., Wise, K. E., Lowther, S. E., et al. 2015. "Multifunctional Electroactive Nanocomposites Based on Piezoelectric Boron Nitride Nanotubes." *Acs Nano* 9 (12): 11942-50.

[13] Chandra, A., Patra, P. K., and Bhattacharya, B. 2016. "Thermomechanical Buckling of Boron Nitride Nanotubes Using Molecular Dynamics." *Materials Research Express* 3 (2): 025005.

[14] Huang, Y., Lin, J., Zou, J., Wang, M. S., Faerstein, K., Tang, C., et al. 2013. "Thin Boron Nitride Nanotubes with Exceptionally High Strength and Toughness." *Nanoscale* 5 (11): 4840-6.

[15] Li, T., Tang, Z., Huang, Z., and Yu, J. 2017. "A Comparison between the Mechanical and Thermal Properties of Single-Walled Carbon Nanotubes and Boron Nitride Nanotubes." *Physica E: Low-Dimensional Systems and Nanostructures* 85: 137-42.

[16] Kinoshita, Y., and Ohno, N. 2010. "Electronic Structures of Boron Nitride Nanotubes Subjected to Tension, Torsion and Flattening: A First-Principles DFT Study." *Physical Review B* 82 (8): 085433.

[17] Anoop Krishnan, N., and Ghosh, D. 2014. "Defect Induced Plasticity and Failure Mechanism of Boron Nitride Nanotubes under Tension." *Journal of Applied Physics* 116 (4): 044313.

[18] Anoop Krishnan, N., and Ghosh, D. 2014. "Chirality Dependent Elastic Properties of Single-Walled Boron Nitride Nanotubes under Uniaxial and Torsional Loading." *Journal of Applied Physics* 115 (6): 064303.

[19] Xiong, Q. L., and Tian, X. G. 2015. "Torsional Properties of Hexagonal Boron Nitride Nanotubes, Carbon Nanotubes and Their Hybrid Structures: A Molecular Dynamics Study." *AIP Advances* 5 (10): 107215.

[20] Garel, J., Leven, I., Zhi, C., Nagapriya, K. S., Popovitz-Biro, R., Golberg, D., et al. 2012. "Ultrahigh Torsional Stiffness and Strength of Boron Nitride Nanotubes." *Nano Letters* 12 (12): 6347-52.

[21] Tanur, A. E., Wang, J., Reddy, A. L., Lamont, D. N., Yap, Y. K., and Walker, G. C. 2013. "Diameter-Dependent Bending Modulus of Individual Multiwall Boron Nitride Nanotubes." *The Journal of Physical Chemistry B* 117 (16): 4618-25.

[22] Zhang, J. 2016. "Size-Dependent Bending Modulus of Nanotubes Induced by the Imperfect Boundary Conditions." *Scientific Reports* 6.

[23] Hollerer, S. 2014. "Numerical Validation of a Concurrent Atomistic-Continuum Multiscale Method and Its Application to the Buckling Analysis of Carbon Nanotubes." *Computer Methods in Applied Mechanics and Engineering* 270: 220-46.

[24] Wang, C. G., Liu, Y. P., Al-Ghalith, J., Dumitrică, T., Wadee, M. K., and Tan, H. F. 2016. "Buckling Behavior of Carbon Nanotubes under Bending: From Ripple to Kink." *Carbon* 102: 224-35.

[25] Tersoff, J. 1989. "Modeling Solid-State Chemistry: Interatomic Potentials for Multicomponent Systems." *Physical Review B* 39 (8): 5566.

[26] Sevik, C., Kinaci, A., Haskins, J. B., and Çağın, T. 2011. "Characterization of Thermal Transport in Low-Dimensional Boron Nitride Nanostructures." *Physical Review B* 84 (8): 085409.

[27] Liu, B., Huang, Y., Jiang, H., Qu, S., and Hwang, K. C. 2004. "The Atomic-Scale Finite Element Method." *Computer Methods in Applied Mechanics and Engineering* 193 (17): 1849-64.

[28] Wackerfuß, J. 2009. "Molecular Mechanics in the Context of the Finite Element Method." *International Journal for Numerical Methods in Engineering* 77 (7): 969-97.

[29] Le, M. Q., and Nguyen, D. T. 2014. "Atomistic Simulations of Pristine and Defective Hexagonal BN and SiC Sheets under Uniaxial Tension." *Materials Science & Engineering A* 615: 481-8.

[30] Le, M. Q. 2014. "Atomistic Study on the Tensile Properties of Hexagonal AlN, BN, GaN, InN and SiC Sheets." *Journal of Computational and Theoretical Nanoscience* 11 (6): 1458-64.